# Measurement of the Translational and Rotational Brownian Motion of Individual Particles in a Rarefied Gas

Jürgen Blum,* Stefan Bruns, Daniel Rademacher, Annika Voss, Björn Willenberg, and Maya Krause

*Institut für Geophysik und Extraterrestrische Physik, Technische Universität Braunschweig, Mendelssohnstraße 3, 38114 Braunschweig, Germany*

(Received 2 August 2006; published 4 December 2006)

We measured the free Brownian motion of individual spherical and the Brownian rotation of individual nonspherical micrometer-sized particles in rarefied gas. Measurements were done with high spatial and temporal resolution under microgravity conditions in the Bremen drop tower so that the transition from diffusive to ballistic motion could be resolved. We find that the translational and rotational diffusion can be described by the relation given by Uhlenbeck and Ornstein [Phys. Rev. **36**, 823 (1930)]. Measurements of rotational Brownian motion can be used for the determination of the moments of inertia of small particles.

DOI: 10.1103/PhysRevLett.97.230601 PACS numbers: 05.40.Jc, 47.45.Ab, 47.50.Ef

The Brownian motion of small solid particles was first described by Brown in 1828 [1]. The thermodynamical description of the Brownian motion as a result of energy equipartition between all participating entities was given by Einstein in 1905 [2]. Einstein showed that the diffusion constant $D$, which is observable through the widening of an initially sharp probability distribution function $p(\Delta x, \Delta t)$, following a Gaussian evolution law

$$p(\Delta x, \Delta t) = \frac{1}{\sqrt{4\pi D \Delta t}} \exp\left(\frac{-(\Delta x)^2}{4D\Delta t}\right), \tag{1}$$

can be formulated by

$$D = \frac{kT}{f}. \tag{2}$$

Here, $\Delta x$, $\Delta t$, $k$, and $T$ are the spatial and temporal variables, Boltzmann's constant, and the temperature of the gas and particles. In a rarefied gas environment, in which the mean free path of the gas molecules exceeds the particle size, the friction coefficient $f$ in Eq. (2) is given by a weighted sum of a component based upon specular molecule reflection, $f_{\mathrm{sp}}$, and a component depending on diffuse scattering of molecules, $f_{\mathrm{di}}$ [3],

$$f = g f_{\mathrm{sp}} + (1 - g) f_{\mathrm{di}}, \tag{3}$$

with

$$f_{\mathrm{sp}} = \frac{4}{3} \pi s^2 \rho_g v_m \tag{4}$$

and

$$f_{\mathrm{di}} = f_{\mathrm{sp}}\left(1 + \frac{\pi}{8}\right). \tag{5}$$

Besides the distinction between the two types of particle-gas interaction through the parameter $g \in [0, 1]$, the strength of the particle friction in the Epstein gas-drag regime is determined by the particle radius $s$, the mass density of the gas $\rho_g$, and the mean molecular velocity $v_m$, which is given by $v_m = \sqrt{\frac{8kT}{\pi m_m}}$, with $m_m$ being the mass of the gas molecules. It is obvious from Eq. (4) that the interaction between gas and particles in free-molecular flow regime is determined by the geometric cross section $\pi s^2$ of the solid particle.

For a single particle, the diffusion constant can be measured through the mean square displacement of the particle position in one dimension, $\langle \Delta x^2 \rangle$, within a time interval $\Delta t$ by

$$D = \frac{\langle \Delta x^2 \rangle}{2\Delta t}. \tag{6}$$

Equation (6) is, however, valid only in the limit $\Delta t \gg \tau_f$. Here, $\tau_f$ is the particle's response time to a relative motion between gas and particle and is given by

$$\tau_f = \frac{m}{f} \tag{7}$$

with $m$ being the mass of the solid particle.

For short observation times $\Delta t \ll \tau_f$, a solid particle cannot follow the gas motion, so its path should be determined by the particle's inertia. A solution to the Langevin equation for arbitrary times was given by Uhlenbeck and Ornstein [4],

$$\langle \Delta x^2 \rangle = 2D\Delta t\left(1 - \frac{\tau_f}{\Delta t} + \frac{\tau_f}{\Delta t} \exp\left[-\frac{\Delta t}{\tau_f}\right]\right), \tag{8}$$

which has the two limiting cases $\langle \Delta x^2 \rangle = 2D\Delta t$ for $\Delta t \gg \tau_f$ and $\langle \Delta x^2 \rangle = (\Delta t)^2 \frac{kT}{m}$ for $\Delta t \ll \tau_f$. If we define for $\Delta t \ll \tau_f$ the one-dimensional particle velocity by $v_x = \frac{\sqrt{\langle \Delta x^2 \rangle}}{\Delta t}$, we get for the one-dimensional kinetic energy of the solid particle $E_x = \frac{1}{2} m v_x^2 = \frac{1}{2} kT$, i.e., the well-known equipartition of energy in thermodynamics. Equation (8) assumes no feedback from the particle to the fluid motion so that hydrodynamic memory effects, as otherwise observed [5], are negligible. If high-precision data on particle

 © 2006 The American Physical Society

size, gas density, and temperature are available, the measurement of the particle diffusivity in the free-molecular flow regime and the application of Eqs. (2)–(5) allow the determination of the microphysical parameter $g$ in Eq. (3).

As the energy equipartition should be given for all degrees of freedom in particle motion, we expect the existence of a relation equivalent to Eq. (8) for the rotational motion of the particle. Substituting the particle mass $m$ by its moment of inertia $\Theta$, the square spatial displacement $\langle \Delta x^2 \rangle$ by its one-dimensional angular counterpart $\langle \Delta \vartheta^2 \rangle$, and the gas-particle response time for translational motion $\tau_f$ by the response time for rotational motion $\tau_r$, we get in analogy to Eq. (8) for the rotational motion of a particle

$$\langle \Delta \vartheta^2 \rangle = 2D_r \Delta t \left( 1 - \frac{\tau_r}{\Delta t} + \frac{\tau_r}{\Delta t} \exp\left[ -\frac{\Delta t}{\tau_r} \right] \right), \qquad (9)$$

with the rotational diffusion constant $D_r$ given by

$$D_r = \frac{kT\tau_r}{\Theta}. \qquad (10)$$

For $\Delta t \ll \tau_r$, Eq. (9) transfers to $\langle \Delta \vartheta^2 \rangle = (\Delta t)^2 \frac{kT}{\Theta}$. If we define for $\Delta t \ll \tau_r$ the angular particle velocity by $\omega = \frac{\sqrt{\langle \Delta \vartheta^2 \rangle}}{\Delta t}$, we get for the one-dimensional rotation energy of the solid particle $E_r = \frac{1}{2}\Theta\omega^2 = \frac{1}{2}kT$.

While the translational Brownian motion of individual micrometer-sized particles in rarefied gases was measured before with high spatial ($\sim 1$ $\mu$m) and medium temporal ($\tau \gtrsim \Delta t$) resolution [6–8], the rotational Brownian motion has not been observed for individual free particles. Earlier work on Brownian rotation used colloidal particles and concentrated on cumulative effects [9].

For the visualization of the translational Brownian motion of free particles at high temporal ($\tau_f \approx \Delta t$) and spatial ($\sim 1$ $\mu$m) resolution, we used silica ($SiO_2$) particles with a narrow size distribution around a radius of $s = 0.76$ $\mu$m. To visualize the rotational motion, we chose commercially available SiC whiskers with typical diameters of $\sim 1$ $\mu$m and lengths in the range 10–100 $\mu$m (Fig. 1). The particles were suspended within rarefied air of typically 100 Pa pressure. For the deagglomeration and dispersion of the $SiO_2$ and SiC particles, we used the fast-rotating cogwheel technique [10,11]. Observation of the particle motion was done by a long-distance microscope [7,8,12] with an attached high-speed complementary metal oxide semiconductor camera. The camera can record 462 frames per second (fps) with $1024 \times 1024$ pixel resolution and 924 fps with $1024 \times 512$ pixel resolution. Thus, we get a typical temporal resolution of $\sim$1–2 ms. The spatial resolution of the long-distance microscope was $\sim 1$ $\mu$m. The magnification of the microscope resulted in a field of view of $0.67 \times 0.67$ mm$^2$ (462 fps) and $0.67 \times 0.33$ mm$^2$ (924 fps), respectively. The depth of focus of the optical setup was $\sim 80$ $\mu$m. The illumination of the field of view was reached by the bright-field technique using Xenon flash lamps with a duration of a single light flash of $\sim 1$ $\mu$s.

As the sedimentation velocity of the particles exceeds their thermal velocity by far and as a sedimentational motion can cause unwanted drift and rotation, we performed the experiments under microgravity conditions (residual acceleration $< 10^{-5}$ m s$^{-2}$) in the Bremen drop tower. The total duration of the microgravity phase in the drop tower is 4.74 s.

We performed five microgravity experiments on the translational Brownian motion with dispersions of spherical $SiO_2$ particles and measured the particle positions with an accuracy of better than 1 $\mu$m. The temporal resolution of these measurements was 2.16 ms. Figure 2 shows the trajectory of a single $SiO_2$ sphere [13]. The one-dimensional displacements of the particle in Fig. 2 are shown in Fig. 3(a) for three different time steps $\Delta t$. The solid lines are the best-fitting Gaussians to the data following Eq. (1). It can be clearly seen that with increasing $\Delta t$ the width of the Gaussian probability distribution increases. Figure 4 shows the dependence of the mean square displacement of the $SiO_2$ particle from Fig. 2 on the time interval between two observations. The solid line in Fig. 4 is a fit of Eq. (8) to the data. The resulting fit parameters are $D = 1.3 \times 10^{-9}$ m$^2$ s$^{-1}$ and $\tau_f = 1.7 \times 10^{-3}$ s. The agreement between the prediction of Eq. (8) and our data is excellent. The deviation from the $\langle \Delta x^2 \rangle = 2D\Delta t$ rela-

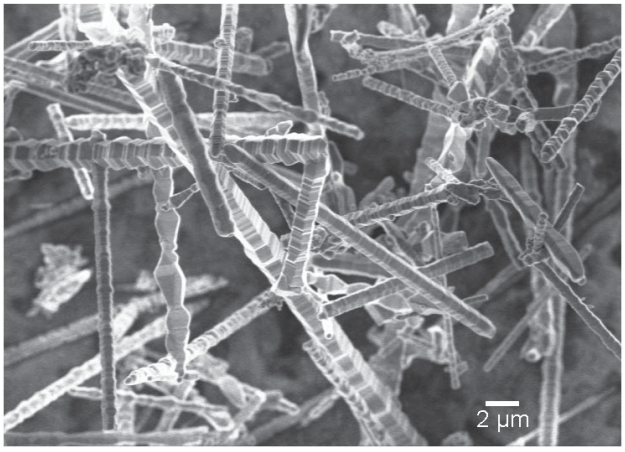


FIG. 1. Scanning electron microscopy image of the SiC particles used for the measurements of Brownian rotation.

FIG. 2. Trajectory of a single $SiO_2$ sphere with $s \approx 0.8$ $\mu$m radius [13]. The trajectory consists of 1024 measurements (black points) and spans a total of 2.2 s. The scale bar indicates 10 $\mu$m.

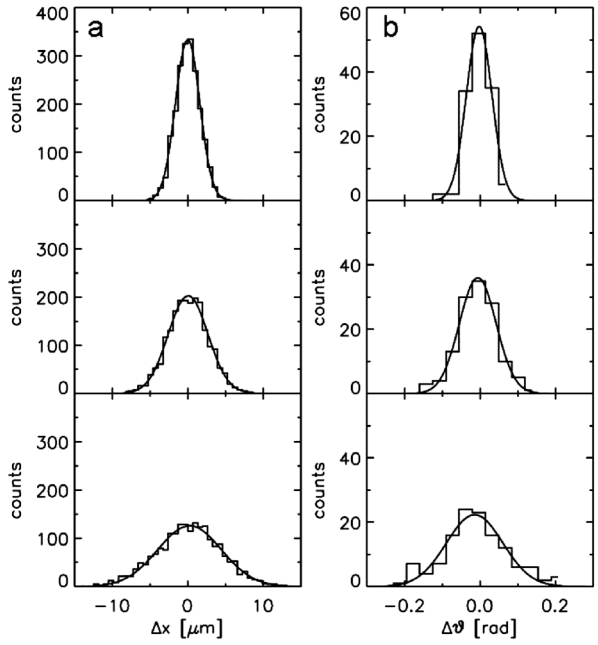


FIG. 3. (a) Histogram of the one-dimensional motion of the $SiO_2$ particle in Fig. 2 for the time steps (from top to bottom) $\Delta t = 1 \times \Delta t_0$, $2 \times \Delta t_0$, $4 \times \Delta t_0$ with $\Delta t_0 = 2.16$ ms. (b) Histogram of the one-dimensional rotation of the SiC particle in Fig. 5 for the time steps (from top to bottom) $\Delta t = 1 \times \Delta t_0$, $2 \times \Delta t_0$, $4 \times \Delta t_0$ with $\Delta t_0 = 1.08$ ms. The solid curves in (a) and (b) are best-fitting Gaussians.

tion can be clearly seen for the shortest observation times for which $\tau_f \approx \Delta t$. As the main objective of this study was to show the feasibility of precision measurements of particle diffusion in rarefied gas, we used a noncalibrated pressure sensor so that the derivation of the coefficient $g$ in Eq. (3) was not possible.

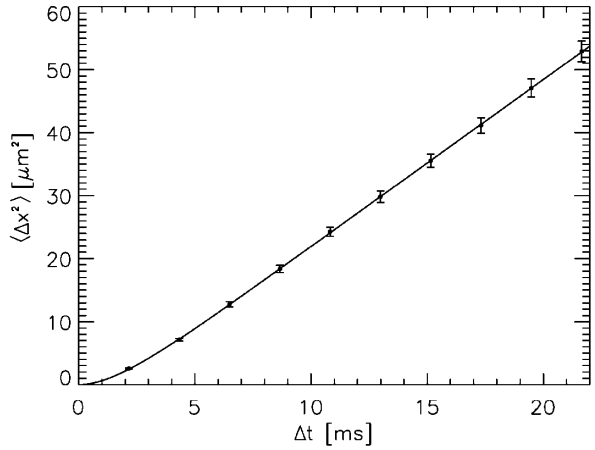


FIG. 4. Mean square one-dimensional displacement of the particle in Fig. 2 as a function of the time interval between measurements (data points with error bars). The solid line is the best-fitting relation following Eq. (8) for the translational Brownian motion.

With Eqs. (2) and (7) and $T = 300$ K, we can calculate the expected particle mass through $m = \frac{kT\tau_f}{D} = 5.4 \times 10^{-15}$ kg. With a mass density of $\rho_{SiO_2} = 2200\ \mathrm{kg\,m^{-3}}$ for the $SiO_2$ particles, we get an expected particle radius of $s = \sqrt[3]{\frac{3m}{4\pi\rho_{SiO_2}}} = 0.84\ \mu$m. This particle radius is in agreement with the measured radius distribution function [14] so that we can conclude that our measurements are consistent with the predictions by Eq. (8).

Among the ten microgravity experiments with SiC whiskers, we were able to find only one particle that consisted of a single whisker so that one-dimensional rotational diffusion can be easily measured. As can be seen in Fig. 1, the SiC whiskers seem to be welded together at their outer tips so that the deagglomeration was rather unsuccessful and most particles consisted of more than one whisker [13]. However, the one linear particle which we found was rather well focused and visible in 349 successive images (corresponding to a total duration of 0.38 s). Figure 5 shows some snapshots of its rotational motion [13]. Equation (9) describes the rotational Brownian motion in one dimension only and assumes a constant diffusivity $D_r$. As can be seen in Eq. (10), the diffusion constant depends on the particle orientation and rotation axis through the moment of inertia and the rotational gas-grain coupling time. Thus, we chose a part of the rotational trajectory of the particle in which the rotation axis was rather stable, i.e., in which the projected length of the SiC particle did not change substantially. Because of this restriction, the number of successive images was 131 and the total duration of the rotational trajectory was 0.14 s. As the selected (constant) length was the maximum measured in the whole observation period, we assume that the projected length corresponds to the real length of the SiC whisker.

We then measured the angular orientation $\vartheta$ of the long axis in each image. Subsequently, we determined the angle differences $\Delta\vartheta$ for the time intervals $\Delta t = it_0$,

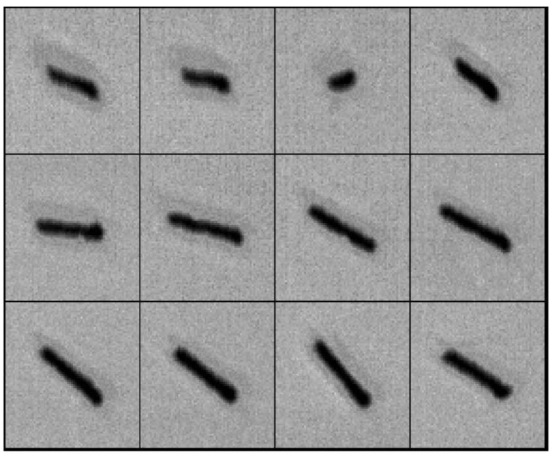

FIG. 5. Snapshots of the orientation of a SiC whisker during a microgravity experiment [13]. The displayed frames show each 18th image and were recorded at time steps of 19.5 ms. The size of each image is $47 \times 47\ \mu\mathrm{m}^2$.

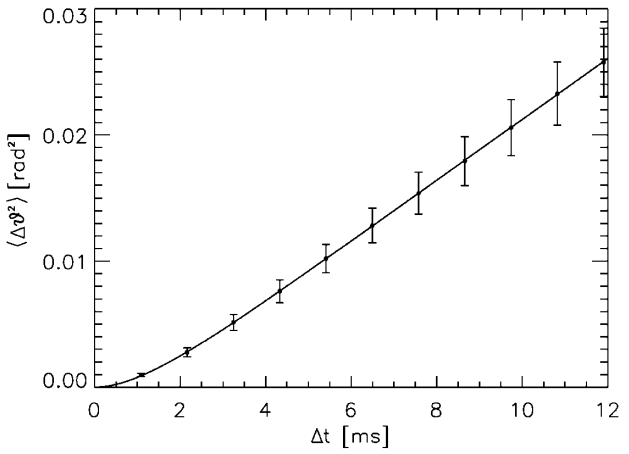


FIG. 6. Mean square angular displacement as a function of the time interval between measurements (data points with error bars). The solid line is the best-fitting relation after Eq. (9) for the rotational Brownian motion.

with $i = 1, 2, 3, \ldots, 11$ and $t_0 = \frac{1}{924}$ s $= 1.08 \times 10^{-3}$ s. Figure 3(b) shows these data for three different sampling times $\Delta t$. The solid curves are fitted Gaussians. As in the translational case [see Fig. 3(a)], the distribution gets wider with increased sampling time. Figure 6 shows the dependence of the mean square angular displacement $\langle \Delta\vartheta^2 \rangle$ on $\Delta t$. It can be clearly seen that for $\Delta t \gtrsim 5$ms we have a linear relation between the mean square angular displacement and the measurement time interval. For $\Delta t \gg \tau_r$, we can approximate Eq. (9) to

$$\langle \Delta\vartheta^2 \rangle = 2D_r \Delta t \left(1 - \frac{\tau_r}{\Delta t}\right) = 2D_r(\Delta t - \tau_r), \qquad (11)$$

which is a linear relation with a slope of $2D_r$ and an intersection with the $\langle \Delta\vartheta^2 \rangle = 0$ line at $\Delta t = \tau_r$. A fit of the data in Fig. 6 to Eq. (9) gives $D_r = 1.2\ \mathrm{s}^{-1}$ and $\tau_r = 1.2 \times 10^{-3}$ s. The agreement between the data in Fig. 6 and Eq. (9) is very good. As there is no theoretical estimation of the gas-grain coupling time for rotational motion known, we can only state that the $\tau_r$ value seems not implausible. With the knowledge of the ambient temperature ($T = 300$ K) we can measure the moment of inertia of small particles. Using the fit results shown above, we get for the moment of inertia of our SiC whisker $\Theta = 4.14 \times 10^{-24}\ \mathrm{kg\,m^2}$. We can use this value and derive from that the radius $s$ of the SiC rod. The moment of inertia of a long rod is given by $\Theta = \frac{1}{12} m l^2 = \frac{\pi}{12} \rho_{\mathrm{SiC}} s^2 l^3$. With a measured length of $l = 24.8\ \mu$m and a mass density of SiC of $\rho_{\mathrm{SiC}} = 3217\ \mathrm{kg\,m^{-3}}$, we get for the radius $s = 0.57\ \mu$m, which is a very plausible value.

We have presented the first high-resolution data of the transition range between ballistic and diffusive translational and rotational Brownian motion of free particles in rarefied gas. The mean square spatial and angular displacements can be described by Eq. (8) for translation and by Eq. (9) for rotation. Measurement of the time-resolved angular motion of fine particles allows the determination of the moments of inertia and the rotational gas-grain coupling time. Applications for Brownian rotation can be found in astrophysics where the thermal rotation influences the structure of dust aggregates [8,15]. In addition to that, grain alignment plays an important role in the interpretation of interstellar polarization measurements [16] where Brownian rotation can act against grain alignment by magnetic fields.

This work was part of a microgravity training program for students at the Physics Faculty of Braunschweig Technical University and was supported by the German Space Agency (DLR) under Contract No. 50WM0336. We thank Lars Heim from the Max Planck Institute for Polymer Research in Mainz for the scanning electron microscopy image of the SiC particles.

*To whom correspondence should be addressed.
Electronic address: j.blum@tu-bs.de

[1] R. Brown, Edinburgh New Philos. J. **5**, 358 (1828).
[2] A. Einstein, Ann. Phys. (Berlin) **17**, 549 (1905).
[3] P. S. Epstein, Phys. Rev. **23**, 710 (1924).
[4] G. E. Uhlenbeck and L. S. Ornstein, Phys. Rev. **36**, 823 (1930).
[5] B. Lukič, S. Jeney, C. Tischer, A. J. Kulik, L. Forró, and E.-L. Florin, Phys. Rev. Lett. **95**, 160601 (2005).
[6] J. Blum, G. Wurm, S. Kempf, and T. Henning, Icarus **124**, 441 (1996).
[7] J. Blum *et al.*, Phys. Rev. Lett. **85**, 2426 (2000).
[8] M. Krause and J. Blum, Phys. Rev. Lett. **93**, 021103 (2004).
[9] S. Broersma, J. Chem. Phys. **32**, 1626 (1960); M. Mercedes Tirado, C. López Martínez, and J. García de la Torre, J. Chem. Phys. **81**, 2047 (1984); J. J. Magda, H. T. Davis, and M. Tirrell, J. Chem. Phys. **85**, 6674 (1986); J. Kanetakis, A. Tölle, and H. Sillescu, Phys. Rev. E **55**, 3006 (1997).
[10] T. Poppe, J. Blum, and T. Henning, Rev. Sci. Instrum. **68**, 2529 (1997).
[11] J. Blum and R. Schräpler, Phys. Rev. Lett. **93**, 115503 (2004).
[12] J. Blum *et al.*, Meas. Sci. Technol. **10**, 836 (1999).
[13] See EPAPS Document No. E-PRLTAO-97-030649 for further information. For more information on EPAPS, see http://www.aip.org/pubservs/epaps.html.
[14] T. Poppe and R. Schräpler, Astron. Astrophys. **438**, 1 (2005).
[15] D. Paszun and C. Dominik, Icarus **182**, 274 (2006).
[16] A. Lazarian, A. A. Goodman, and P. C. Myers, Astrophys. J. **490**, 273 (1997); A. Lazarian and J. Cho, Astron. Soc. Pac. Conf. Ser. **343**, 333 (2005).